

Quantification of triglyceride fatty acid composition in the fatty liver, subcutaneous and visceral adipose tissues with 3.0T MRI.

Benjamin Leporq¹, Simon Auguste Lambert¹, Hélène Ratiney², Gaspard D'Assignies^{1,3}, Maxime Ronot^{1,3}, Valérie Vilgrain^{1,3}, Olivier Beuf², and Bernard Van Beers^{1,3}

¹Center for research on inflammation, Université PARIS 7 ; INSERM U1149, Paris, France, ²CREATIS CNRS UMR 5220; INSERM U1044; INSA Lyon; UCBL Lyon 1, Université de Lyon, Villeurbanne, France, ³Beaujon hospital; Department of radiology, Assistance Publique Hopitaux de Paris, Clichy, France

Introduction: In the past decade, the rise of incidence of obesity, diabetes and lipid metabolism disorders has triggered an epidemic increase of Non-Alcoholic Fatty Liver Diseases (NAFLD) prevalence. NAFLD is among the most common causes of chronic liver disease with a prevalence ranging between 17 and 46% (1). Nonalcoholic steatohepatitis (NASH) is a part of the NAFLD spectrum which, in addition to presence of excess fat in the liver (steatosis), is accompanied by liver inflammation with hepatocyte injury (ballooning) with or without fibrosis. NASH can progress to cirrhosis, liver failure, hepatocellular carcinoma and may require transplantation. There is thus a clinical need for non-invasive quantification methods of liver fat content. Advanced chemical-shift based methods have been shown to be accurate for the quantification of liver fat (2,3). Nevertheless, these methods cannot separate between NASH and simple steatosis whereas the noninvasive distinction between these two forms constitutes a very important clinical need. Using gas chromatography analysis in ex-vivo SREBP-1 rat liver (4) and in humans (5), it has been shown that the modifications in liver fatty acid (FA) composition (depletion of polyunsaturated FA and disturbance in the saturated to unsaturated FA ratio) plays a role in the pathophysiology of NASH. Our study aimed to validate a method for quantifying the FA composition in the fatty liver, in the subcutaneous (SAT) and visceral (VAT) adipose tissues at 3.0T MRI.

Methods: MR acquisition: Acquisitions were performed on a Philips Ingenia 3.0T (*Philips, Best, The Netherlands*) using a 3D spoiled-gradient multiple echo sequence with parallel imaging employing sensitivity encoding and multi transmit parallel radiofrequency transmission. The acquisition parameters were: TR/flip angle, 10 ms/3°; SENSE factors, 1.5 and 1.8 according to slice and phase direction respectively; receiver bandwidth, 2000 Hz.pixel⁻¹; FOV, 420 × 380 × 160 mm³; acquisition matrix, 140 × 128 × 40 (256² rebuilding) and 2 signal averages. Forty slices of 4 mm thickness in the transverse plane were acquired using eight echoes: n × 1.15 ms with n = 1,...,8. Total scan duration was 20 s. Phase and magnitude images were saved. **Quantification algorithm:** Native phase images were corrected for wrap, zero- and first-order phase to rebuild the real part images. Then, using a model built upon a fat ¹H MR spectrum integrating nine components, the number of protons was expressed according to the averaged number of double bonds (ndb), the mean chain length (CL) and the mean number of methylene interrupted double bonds (nmidb) (6), these parameters were derived. FA composition was deduced according to: polyunsaturated FA fraction, F_{PUFA} = nmidb/3; monounsaturated FA fraction, F_{MUFA} = (ndb - 2 × nmidb)/3; and saturated FA fraction, F_{SFA} = 1-(F_{PUFA}+F_{MUFA}). **Phantom experiments:** A phantom was made by filling eight vials with different oils (olive, sesame, sunflower, walnuts, peanuts, hazelnuts, grape seed and canola) immersed in a sonographic gel. The phantom was scanned with the above described MR protocol. **In vivo experiments:** Two healthy obese volunteers (1 M, 1 W; mean age: 29.5 ± 3.5 years; mean body mass index: 35.4 ± 1.9 kg.m⁻²) had an MRI examination with the same MRI protocol.

Results

Oil	ndb		nmidb		CL		PDFF (%)	T ₂ * (ms)
	Theory	Measured	Theory	Measured	Theory	Measured		
Peanut	3.39	3.18 ± 0.29	1.01	1.15 ± 0.30	17.97	17.60 ± 0.12	99.7 ± 0.6	43.5 ± 5.7
Canola	3.98	3.72 ± 0.19	1.05	1.17 ± 0.16	17.95	17.74 ± 0.04	98.9 ± 1.0	39.9 ± 6.1
Sunflower	4.59	4.25 ± 0.19	1.95	1.68 ± 0.20	17.90	17.86 ± 0.05	97.5 ± 1.5	33.7 ± 5.0
Olive	2.86	2.90 ± 0.27	0.32	0.72 ± 0.20	17.74	17.52 ± 0.05	98.8 ± 1.0	45.3 ± 6.3
Walnut	5.40	5.10 ± 0.19	2.32	2.22 ± 0.23	17.84	18.06 ± 0.05	95.3 ± 2.4	21.9 ± 2.9
Sesame	3.89	3.71 ± 0.36	1.32	1.50 ± 0.34	17.80	17.72 ± 0.09	99.8 ± 0.5	36.1 ± 4.1
Hazelnut	3.05	3.12 ± 0.38	0.27	0.82 ± 0.35	17.91	17.58 ± 0.09	99.6 ± 0.7	36.1 ± 4.8
Grape seed	4.98	4.68 ± 0.30	2.18	1.92 ± 0.22	17.90	17.94 ± 0.04	97.3 ± 2.1	29.3 ± 4.7

Tab.1: Proton density fat fraction (PDFF) and T₂* measured in each vial. Theoretical FA composition-related parameters (ndb, nmidb and CL) of each oil calculated from FA mass composition and used as a reference for the in vitro study.

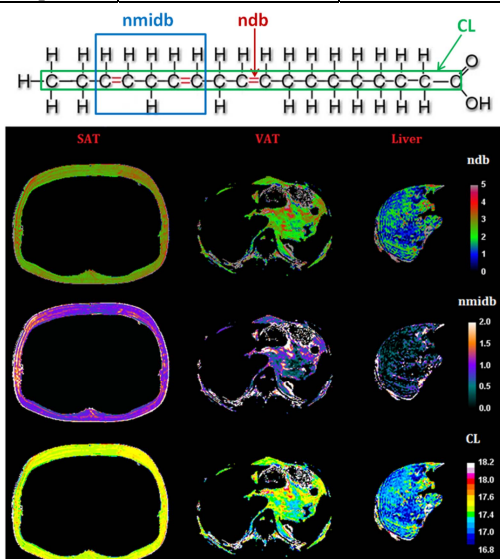


Fig.1 FA composition-related parametric maps: ndb, nmidb and CL in SAT, VAT and liver performed on an obese subject. These maps are derived from native parametric maps after the application of a 4-cluster mask to segment SAT, VAT, and liver.

References

- (1) Ratiu V et al. J Hepatol 2010;53:372-84
- (4) Malinska et al. Mol Cell Biochem 2010; 335:119-25.
- (7) Ren J et al. J Lipid Res 2008;49:2055.
- (10) Bydder M et al. Magn Reson Imag 2011;29:1041-1046.
- (2) Hines C et al. J Magn Reson Imaging 2011;33:873-881.
- (5) Allard J.P et al. 2008;48:300-307.
- (8) Hodson L et al. Prog Lipid Res 2008;47:348-380.
- (3) Leporq B et al. Eur Radiol 2013;23:2175-2186.
- (6) Hamilton G et al. NMR biomed 2011;24:784-79
- (9) Peterson P et al. Magn Reson Med 2013;69:688-697.

The linear regressions between measured and theoretical values were $y=0.86x+0.4$; $r^2=0.99$; $p<0.0001$ and $y=0.65x+0.54$; $r^2=0.96$; $p<0.0001$ for ndb and nmidb respectively. Mean T₂* were: 15.7 ± 2.7, 35.6 ± 12.6 and 24.6 ± 0.9 ms in liver, SAT and VAT respectively. Mean PDFF were 28.6 ± 0.90%, 93.0 ± 0.78%, and 84.3 ± 1.76% in liver, SAT and VAT respectively. Mean ndb/nmidb/CL were: 1.64 ± 0.26 / 0.65 ± 0.20 / 17.23 ± 0.05; 2.68 ± 0.36 / 0.93 ± 0.08 / 17.46 ± 0.08 and 2.46 ± 0.06 / 0.79 ± 0.02 / 17.41 ± 0.01 in liver, SAT and VAT respectively.

Tissue	F _{PUFA} (%)	F _{MUFA} (%)	F _{SFA} (%)
Liver	21.6 ± 6.6	11.2 ± 4.5	67.2 ± 2.1
SAT	30.8 ± 2.6	27.5 ± 6.8	41.7 ± 9.4
VAT	26.2 ± 0.7	29.4 ± 3.5	44.4 ± 2.3

Tab.2: FA composition (F_{PUFA}, F_{MUFA}, F_{SFA}) measured in the liver, SAT and VAT. Results were presented as mean ± standard deviation.

Discussion: In vitro experiments showed a strong agreement between ndb, nmidb and CL quantified with the experimental method and the theoretical values calculated using oil composition. These results demonstrated the robustness of the sequence and the validity of the data post-processing method to extract ndb, nmidb and CL. In vivo, our results were consistent with previously published data. In abdominal SAT ndb/nmidb/CL were 2.68 ± 0.36 / 0.93 ± 0.08 / 17.46 ± 0.08 in our study vs. 2.89/0.70/17.5 in the study of Ren et al. (7), and 2.69/0.58/17.3 in the review of Hodson et al. (8). The MRI method of Peterson et al (9) also gave similar results (ndb/nmidb/CL 2.83/0.74/18.4). In VAT, ndb measured in our study was in agreement with the measurements of Bydder et al. (10) obtained with a MRI method (2.46 ± 0.06 vs. 2.76). In the fatty liver, our results agreed with those of Hamilton et al. (6) obtained using ¹H MRS (1.64 ± 0.26, 0.65 ± 0.20 and 17.23 ± 0.05 vs. 1.92/0.32/17.45 for ndb, nmidb and CL respectively). Altogether, the proposed method may be used in human subjects as is. A limitation of this method is its sensitivity. Indeed, for small fat fractions, the available signal from fat protons represents only a small portion of the total signal. Therefore, the optimization procedure may be less reliable, and probably fail for low fat fractions.